#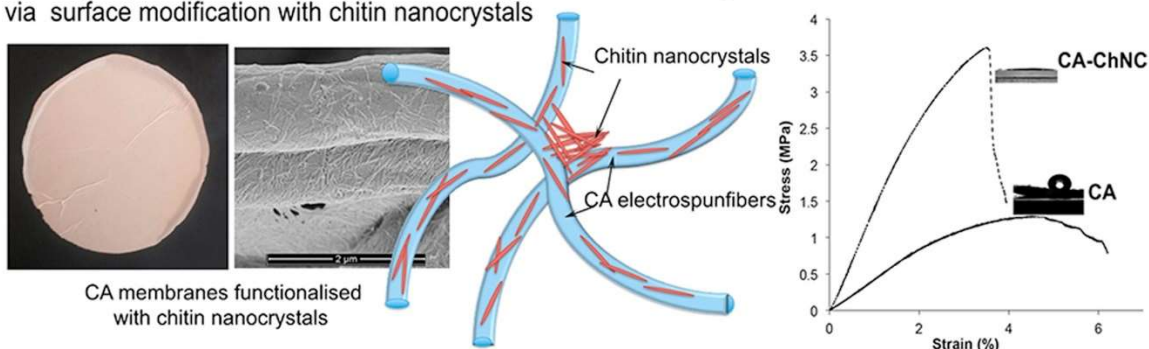 Superhydrophilic anti-fouling electrospun cellulose acetate membranes coated with chitin nanocrystals for water filtration

Superhydrophilic, low-fouling and mechanically enhanced electrospun membranes of cellulose acetate via surface modification with chitin nanocrystals

Superhydrophilic anti-fouling electrospun cellulose acetate membranes coated with chitin nanocrystals for water filtration

Lee A. Goetz[1], Blanca Jalvo[2], RobertoRosal[2], Aji P. Mathew[1,3]

[1] Division of Materials Science, Luleå University of Technology, Luleå 971 87 Sweden
[2] Department of Chemical Engineering, University of Alcalá, Alcalá de Henares E-28871, Madrid, Spain
[3] Department of Materials and Environmental Chemistry, Stockholm University, Stockholm SE-10691, Sweden

* Corresponding author: laura.valenzuela@uah.es

Abstract

Electrospun cellulose acetate (CA) random mats were prepared, and surface coated with chitin nanocrystals (ChNC) to obtain water filtration membranes with tailored surface characteristics. Chitin nanocrystals self-assembled on the surface of CA fibers into homogenous nanostructured networks during drying that stabilized via hydrogen bonding and formed webbed film-structures at the junctions of the electrospun fibers. Coating of CA random mats using 5 % chitin nanocrystals increased the strength by 131 % and stiffness by 340 % accompanied by a decrease in strain. The flux through these membranes was as high as 14200 L m^{-2} h^{-1} at 0.5 bar. The chitin nanocrystal surface coating significantly impacted the surface properties of the membranes, producing a superhydrophilic membrane (contact angle 0 °) from the original hydrophobic CA mats (contact angle 132 °). The coated membranes also showed significant reduction in biofouling and biofilm formation as well as demonstrated improved resistance to fouling with bovine serum albumin and humic acid fouling solutions. The current approach opens an easy, environmentally friendly, and efficient route to produce highly hydrophilic membranes with high water flux and low fouling for microfiltration water purification process wash water from food industry for biological contaminants.

Keywords: Chitin nanocrystals; Electrospinning; Cellulose acetate; Water permeability; Mechanical properties; Anti-fouling.

1. Introduction

Electrospinning is a century old process patented by Cooley and Morton in 1902 that is used for producing continuous fibers [1-2]. The first patent on industrial electrospinning appeared in 1934, where the first commercial equipment for the production of artificial threads/filaments of cellulose acetate was disclosed [3]. Electrospinning is a very versatile technique for producing polymeric fibers in nano- to-micron scale from polymeric solutions and has been of great commercial and research interest. More recently, this technology has been investigated by researchers because of the continuing interest in applications in nanoscience and its potential to generate nanofibers [4-6].

Cellulose acetate-based membranes are used extensively in industrial scale and have the advantage of being derived from the abundant natural polymer cellulose. Though cellulose acetate-based membranes produced by phase inversion is a popular membrane material, electrospun cellulose acetate membranes materials have several advantages, specifically, the open and interconnected pore structure and the large specific surface area while having shown potential in air and water filtration [6-7]. However, membrane filtration and especially pressure-driven liquid filtration using electrospun membranes are challenging due to limitations related to mechanical strength and chemical and thermal stability [8]. Electrospun random mats usually have poor mechanical strength due to the highly porous non-woven structure and with weak fibre–fibre connection via physical entanglements [9]. Process modifications to increase fibre–fibre interactions and reinforcing of electrospun fibers using nanoparticles are becoming a highly promising route to address this issue [10-14]. In addition, biofouling is a significant and constant problem with membrane filtration and specifically for hydrophobic cellulose acetate membranes [15-16]. Methods to address biofouling can include mechanical or chemical cleaning operations but another area of focus is the manipulation of the surface chemistry of the membranes to create a surface inhospitable for biofilm formation [17-18].

In the quest for developing new advanced materials that utilize natural polymers, biobased nanoparticles from cellulose and chitin have been

explored in the last two decades [19-27]. We have successfully reinforced biopolymer fibers electrospun with low (> 10 wt%) and high concentrations (50 wt%) of chitin and cellulose nanocrystals [22], [25-26]. However, it was noticed that addition of nanoparticles to spinning solutions significantly affected the spinnability and process yield which are both significant challenges hindering the use of reinforced fibers in high volume applications such as water purification [26].

Biofouling refers to the undesirable accumulation of a biotic deposit on a surface. This deposition may be due to both macroscopic and microscopic organisms. In contrast to abiotic kinds of fouling (scaling, organic and particle fouling), biofouling is a special case because the foulant, can grow at the expense of biodegradable substances from the water phase, turning them into metabolic products and biomass. "Biofilm" is an expression for a wide variety of manifestations of microbial aggregates [28]. Biofilms are understood to be mixtures of bacterial cells embedded in an extracellular polymeric matrix (EPS) made up of polysaccharides, proteins, and nucleic acids [29]. Biofilm formation is a development process, which initially involves the adhesion of bacterial cells to a surface and production of EPS resulting in more firmly and irreversible bacterial attachment that cover and protect the cells from adverse conditions [30]. The abiotic fouling on the other hand, is the formation of 'cake layer' or 'gel layer' consisting of rejected materials and in membrane filtrations, NOMs are a major contributor for abiotic fouling.

In this current study, chitin nanocrystals are impregnated through electrospun cellulose acetate (CA) in a process to change the surface chemistry of the electrospun fibers. Chitin, poly(β-(1→4)-N-acetyl-D-glucosamine), acts as the structural polymer in the exoskeletons of arthropods, in the cell walls of fungi and yeast, and in other microorganisms [31]. Chitin nanocrystals, rod-like particles with typical dimensions of 400 nm in length and 30 nm in diameter, can be extracted through acid hydrolysis from the above-mentioned sources [32-33]. These nanocrystals have high surface area, good mechanical properties and possess antifungal and antibacterial properties. In a recent study, chitin nanocrystals were successfully incorporated in a PVDF membrane prepared through phase immersion to enhance the anti-fouling performance [34]. The current approach was aimed at combining the ease of producing CA electrospun membranes and its efficiency in

membrane applications with unique surface characteristics of chitin nanocrystals to create a new generation of high flux, super-hydrophilic, anti-fouling composite membranes for microfiltration aimed at water purification for food-processing industries. The fibre morphology, mechanical properties, contact angle, water flux and fouling were evaluated and discussed in this context.

2. Experimental section

2.1. Materials

Cellulose acetate (CA), M_n 50 000, was purchased from Sigma-Aldrich Chemistry, USA. Acetic acid (96 %, EMSURE®), and acetone, analysis grade, were purchased from Merck KGaA (Germany). All chemicals were used as received without further purification.

Chitin nanocrystals (ChNC) were prepared via hydrochloric acid hydrolysis [27], [32-33], [35]. Deproteinized and bleached chitin flakes (Sigma-Aldrich, Germany) underwent an acid hydrolysis reaction with 3 N hydrochloric acid at 80 °C for 90 min. When the reaction was complete, the resulting suspension was centrifuged to remove the excess acid and subsequently to collect the turbid supernatant containing the chitin nanocrystals. This collected fraction, the chitin nanocrystal suspension, was dialyzed against distilled water to achieve a suspension neutral pH and finally sonicated to ensure separation of the individual nanocrystals from one another prior to storage. The chitin nanocrystals suspension was briefly sonicated prior to impregnation on the electrospun cellulose acetate membranes. Concentration of the initial chitin nanocrystals suspension was 0.53 wt%.

2.2. Preparation of electrospun cellulose acetate membranes

A schematic representation of the processing route used to prepare the membranes is given in Fig. 1. Cellulose acetate, 5.0 g (M_n 50 000), was dissolved in a 45 g 1:1 mixture of concentrated acetic acid and acetone and stirred overnight (12 h) to ensure complete dissolution [22]. Electrospinning of the cellulose acetate solution (Fig. 1, step i) was undertaken using the 150 mm Laboratory Electrospinning Platform (Electrospinz-ES1a, New Zealand) attached to a high voltage supplier, with the solution pumped through a 20 mL plastic syringe, (BD Plasti-Pak syringe, USA), using a single syringe pump (Aladdin-1000, World Precision Instrument, USA). The cellulose acetate

fibers were successfully electrospun on aluminium foil on aluminium plates, with a supplied voltage of 10 kV, 150 mm tip to collector distance, and a flow rate of 10 mL h^{-1}. Electrospinning was performed at room temperature.
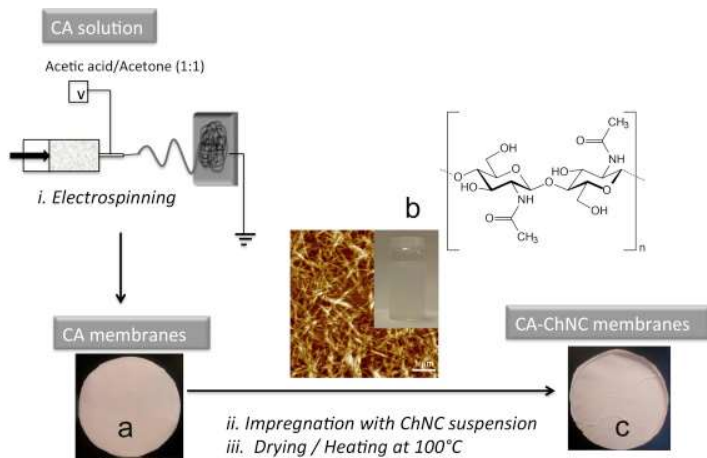

Figure 1. Scheme showing the methods and materials involved in the membrane processing and functionalization. (i) Electrospinning of CA mats, (ii) impregnation of CA mats and (iii) drying and heating of the impregnated mats are the process steps. The (a) electrospun cellulose acetate (CA) mat, (b) chitin nanocrystals (ChNC) used for impregnation (photo of the ChNC suspension, the AFM image of nanocrystals and the chemical structure of chitin) and (c) the CA-ChNC membrane mat obtained after impregnation are shown.

The chitin nanocrystals, with a diameter of 20 nm ± 10 nm and length of 300 nm ± 100 nm, were used to impregnate the CA electrospun mats (Fig. 1, step ii), as shown in Fig. 1. Impregnated membranes (CA-ChNC) were prepared via Buchner funnel filtration apparatus with the cellulose acetate membrane on a 90 mm diameter glass frit. The chitin nanocrystal suspension (0.2 g dry weight, see Fig. 1) was drip fed through the electrospun cellulose acetate fibers. This was to allow for maximum exposure time for the chitin to accumulate on the cellulose acetate fibers. The chitin infused cellulose acetate membranes were air dried for 24 h and then heated to 100 °C for 10 min (Fig. 1, step iii) to ensure binding between the chitin and the cellulose acetate fibers [36-37]. Membranes were weighed on an analytical balance before and after impregnation to determine mass of chitin nanocrystals accumulated on the cellulose acetate mat. 5 % of the total mass of the CA-ChNC mat is due to the ChNC.

The viscosity of the cellulose acetate electrospinning solution was measured using the SV-10 VibroViscometer (A&D Company, Japan) with a glass sample holder. The solution was sampled every 5 s for 2 min at a vibration frequency of 30 Hz. The electrical conductivity of the cellulose acetate electrospinning solution was determined using a SevenEasy™ conductivity meter (METTLER TOLEDO AG, Switzerland).

2.3. Characterization

2.3.1. Membrane porosity and microstructure

Porosity of the scaffolds was evaluated based on the weight and density of the scaffolds. The porosity, υ, was defined as the volume fraction of the voids and calculated using:

$$\upsilon = 1 - \frac{\rho_e}{\rho_t} \qquad (1)$$

where ρ_e is the experimental density of the scaffold and ρ_t is the theoretical density of a non-porous scaffold. The densities of ChNC and cellulose acetate were taken as 1.46 and 1.3 g cm^3, respectively. The experimental density, ρ_e, was determined based on the weight and volume of the samples cut into strips. All reported results are based on the average of three measurements.

The Brunauer–Emmett–Teller (BET) surface area and pore volume of the CA and ChNC-CA membranes were determined by nitrogen adsorption-desorption isotherm measurements at 77 K.

The surface morphology of the electrospun fibers and the membrane were examined using MAGELLAN 400, SEM (FEI Company) or FEG-SEM (Zeiss, Merlin). The fibre samples were placed on conductive tape and sputter coated with tungsten. Images were taken operating at 3 kV and a working distance of 10 mm for MAGELLAN 400, SEM (FEI Company) whereas a 2.5 kV and 8 mm working distance was used in the case of FEG-SEM (Zeiss, Merlin). Post-filtration imaging to observe the continued presence of chitin nanocrystals on the surface of the electrospun CA mats after 5 L distilled water at 0.5 bar pressure was performed with MAGELLAN 400, SEM (FEI Company). The membranes were sputter coated with gold and observed in the SEM at an acceleration voltage of 3 kV.

The chitin nanocrystals as well as CA and CA-ChNC membranes surfaces were imaged using MultiMode 8 AFM (Bruker, Nanoscope controller, Santa Barbara, California, USA). A drop of diluted suspension of each sample was deposited onto freshly cleaved mica and left to dry at room temperature in the case of chitin nanocrystals. In the case of the electrospun membranes, a small piece of the membrane is mounted on the metal stub using double-sided tape. All the samples were imaged in tapping mode. Height, amplitude, and phase images were recorded. The instrument was operated at a resonance frequency of 350 kHz and a spring constant of 10–200 nm^{-1}.

2.3.2. Mechanical properties

The tensile tests were performed on the CA and CA-ChNC mats using a universal testing machine, Shimadzu Autograph AG-X (Shimadzu, Japan), with a load cell 500 N. The thickness of the mats was determined using SEM imaging of the cross-section of cryo-fractured films, sputter coated with Au. Test specimens, conditioned at 45 % relative humidity for 1

week, with dimensions of 50 × 5 mm was mounted on paper windows for ease of handling and mounting. A preload of 0.1 N was applied and a strain rate of 2 mm/min and gauge length of 20 mm were used. The stress–strain curves were plotted from the measured load and sample extension (measured by video camera).

The stress is defined as:

$$\sigma = \frac{F}{A_o} \tag{2}$$

and the strain as:

$$\varepsilon = \ln\left(\frac{L}{L_o}\right) \tag{3}$$

where F is the force at break, A_o is the area of cross-section of the tensile sample, and L_o is the initial sample length and L is the sample length at break. The elastic modulus was calculated from the initial part of the slope from the stress–strain curve. 4–6 test samples were tested for each material and the average values are reported.

2.3.3. Thermal stability

Thermogravimetric analysis was performed using TGA (Q500 TGA, TA Instruments) with 5 mg sample heated to 800 °C at 10 °C min^{-1} under N$_2$ atmosphere. Onset of thermal degradation is the temperature at which 95% of the mass of the original sample remains.

2.3.4. Water flux, permeability, and fouling

Flux tests were performed by filtering distilled water through the membranes using a dead-end cell (HP 4750, Sterlitech, USA) with N$_2$ gas to maintain constant pressure at desired pressures. The time for 0.3 L of distilled water to pass through the membranes was recorded and used for the flux calculations. Flux, J, was calculated as:

$$J = \frac{Q_p}{A_m} \tag{4}$$

where Q_p is the filtrate volume through the membrane per time and A_m is the area of the membrane. A_m (14.6 cm^2) is a constant value provided by Sterlitech. Membranes were compacted at 0.5 bar for 5 min prior to flux experiments. Permeability was calculated from the linear regression slope from plotting the water flux at 0.4–1.2 bar pressure. Correlation factors for both were 0.99.

Anti-fouling capability of the CA and CA-ChNC membranes was determined by measuring the flux decline over time. Bovine serum albumin, fraction V (Merck Millipore, Germany) 2 g L^{-1} stock solution and humic acid (Alfa Aesar, Germany) 0.5 g L^{-1} stock solution were prepared by dissolving the foulant in distilled water and used as prepared. Filtration of the foulant solutions through individual membranes in the dead-end cell occurred at 0.13 bar pressure via a

peristaltic pump (Model 323S, Watson-Marlow, United Kingdom) for 60 min. Every 15 min, the flux at 0.5 bar was measured using the dead-end cell with N$_2$ gas applied to maintain pressure. The flux was plotted against time to determine the effect of the chitin nanocrystals on the surface of the cellulose acetate fibers on fouling and cake formation of the CA and CA-ChNC membranes.

2.3.5. Contact angle measurement

Surface wettability tests were carried out using an optical contact angle meter at room temperature, using the sessile drop technique. For this measurement, the samples were cut and placed on the test cell. Drops of purified water were gently deposited on the sample surface by the delivering syringe. Three water contact angle measurements on each mat surface were taken at different positions on the sample.

2.3.6. Zeta potential measurements

Surface zeta potential was measured via electrophoretic light scattering (Zetasizer Nano ZS) using the Surface Zeta Potential Cell (ZEN 1020) from Malvern. Measurements were performed at 25 °C using 10 mM KCl, pH 7.0, aqueous solution with of 0.5% (w/w) poly (acrylic acid) (450 kDa), as tracer. pH was adjusted using 1 M KOH and 1 M HCl.

2.3.7. Bacterial strain and bioassays

Cells of *Escherichia coli* (CECT 516) were grown overnight in nutrient medium (for 1 L solution in distilled water, beef extract 5 g, peptone 10 g, NaCl 5 g, pH adjusted to 7.2), while shaking at 37 °C. Bacterial viability and biofilm assay were tested using different fluorescence techniques. For these tests, exponentially growing cultures on nutrient medium were diluted to an OD$_{600}$ of 0.0138 (10^8 cells/mL). Diluted cultures (2 mL) were placed on the electrospun CA and CA-ChNC mats inside the well of polystyrene 24-well plates. Mats were incubated 18 and 24 h at 37 °C without stirring. After the biofilm assay, mats were carefully washed with distilled water after the liquid culture removal.

Fluorescein diacetate (FDA), a fluorogenic substrate that permits the detection of enzymatic activity, was used for a relative quantification of the biofilm formation. The fluorescence was measured in a fluorometer/luminometer Fluoroskan Ascent FL. 200 μL of the fluorescent stain were extended over the entire mat surface. A concentration of 0.02% (w/w) in DMSO was used for FDA in all cases. For fluorescence reading, after 15 min of preincubation at 25 °C, FDA was excited at 485 nm, and emission recorded at 538 nm.

DAPI (4′,6-Diamidine-2′-phenylindole dihydrochloride; Roche) and Live/Dead BacLight Bacterial Viability Kit (Molecular Probes, Invitrogen Detection Technologies, Carlsbad, CA, USA) were used to evaluate bacterial viability on mats. For mats staining, the whole surface of each mat was covered with 30 μL of DAPI/PI (2.5

µg/ml DAPI and 30 µM PI in DMSO) or of Live/Dead stain (a 0.5:1 mixture of SYTO 9 and PI in DMSO). The incubation was performed in the dark for 15–30 min at room temperature. For blue fluorescence (DAPI) excitation was performed at 358 nm and emission was recorded at 461 nm. For green fluorescence (SYTO 9) excitation was performed at 488 nm and emission at 500–575 nm. For red fluorescence (PI, dead cells), the excitation/emission wavelengths were 561 nm and 570–620 nm respectively.

For matrix visualization, biofilms were stained with 200 µl FilmTracer SYPRO Ruby (Molecular Probes, Invitrogen) per membrane, incubated in the dark for 30 min at room temperature, and rinsed with distilled water. The excitation/emission wavelengths were 450 nm and 610 nm respectively. After incubation, images were acquired at 18 and 24 h after inoculation in the microdevice using a Leica Microsystems Confocal SP5 fluorescence microscope (Leica Microsystems, Germany).

A process of dehydration and drying with ethanol at different concentrations was carried out to analyse mats in contact with microorganisms by SEM.

3. Results and discussion

3.1. Morphology

Cellulose acetate fibers were successfully electrospun under the given conditions to form random mats. The viscosity and conductivity of the cellulose acetate electrospinning solution were 1144 mPa s and 8.67 mS cm^{-1}, respectively. Fig. 2a shows the electrospun CA fibers where randomly aligned fibrous mats are visible. The electrospun fibers had diameters in the range of 0.5–3.3 µm, with the fibre distribution showing most were between 0.5–1.7 µm (Fig. 2b). The morphology of individual fibres showed ridge-like surfaces (Fig. 2c).

The chitin nanocrystals' dimensions are 20 ± 10 nm diameter and length of 300 ± 100 nm which agrees with out earlier reports [25], [35]. Impregnation of the ChNC on to the surface of the electrospun fibers was undertaken to ensure that the surface functionality of the chitin nanocrystals was utilized and readily accessible. The SEM morphology studies show the hierarchical network formation from the microscale (electrospun fibre networks, Fig. 2d–e) to the nanoscale (ChNC networks, Fig. 2f–g). Fig. 2d shows the overall chitin nanocrystal impregnation network on the surface of the CA fibre random mats, which is extensive even with a relatively low load level of 5% of the mass of the cellulose acetate membrane. The ChNC coatings on the CA fibers (Fig. 2f) were highly homogeneous and were stabilized via H-bonding that was created during the drying step. Ma et al. have used a similar approach to coat TEMPO cellulose nanowhiskers on to electrospun PAN scaffolds on a PET nonwoven substrate [36]. Fig. 2g also shows the build-up and film formation tendency of the chitin nanocrystals in the junctions (crossover) of the electrospun fibers, which reduces the pore sizes

after impregnation. This was shown by the decrease in the porosity of the CA-ChNC membranes when compared to CA membranes, from 88.1% to 85.6%. The average pore diameter decreased from 11.02 nm (CA) to 10.07 nm (CA-ChNC) based on BET measurements. The BET surface area was determined to be 2.73 m^2/g for CA membranes and increased to 3.709 m^2/g with the addition of the 5% ChNC. This increase may be attributed to the nanotexturing of the CA fibers with ChNC.
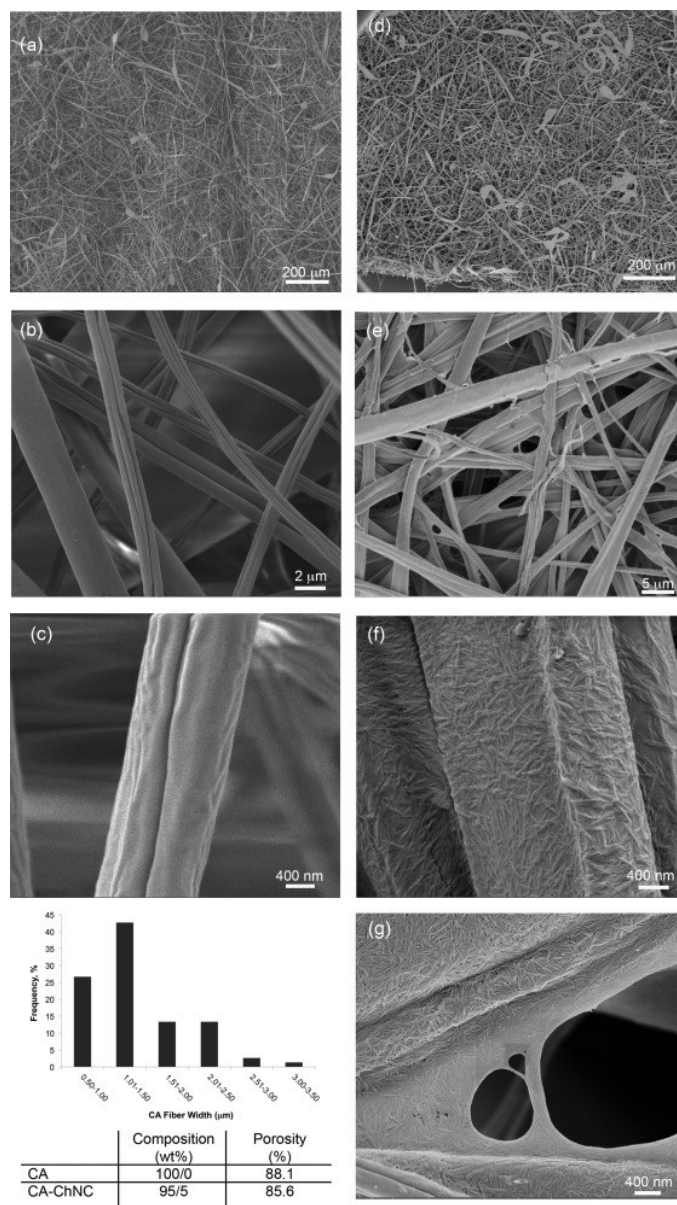

Figure 2. Electrospun cellulose acetate fibers were imaged with SEM to show fibre mat formation (a), surface morphology (b, c) and to determine fibre size distribution (d). After filtration impregnation, the cellulose acetate mat structure is retained (e, f) and the chitin nanocrystals were present both on the surface of the cellulose acetate fibers (g, h) and also formed web-like structures at fibre junctions (g).

To further test the robustness of the chitin nanocrystal layer on the cellulose acetate fibers, 5 L of distilled water at 0.5 bar was passed through the membrane in the dead-end cell. Fig. 3a–b SEM images show that the chitin crystals' webbing between the fibers survives as

well as the chitin crystals coating the individual fibers. The AFM images of a second CA-ChNC membrane that had 26 L distilled water pass through the membrane (Fig. 3c–d) show the chitin nanocrystals on the fibre surfaces also are retained.
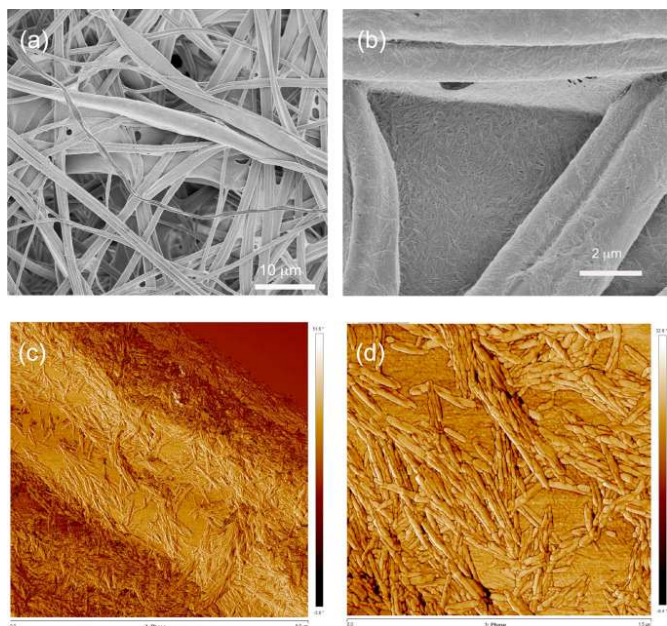

Figure 3. The robustness of the membrane shown by (a) fibre structure and (b–d) chitin crystals on the CA fibers after undergoing 5 L water filtration process. SEM images showing (a) fibre structure and (b) the coated surfaces and ChNC web formations. AFM images showing phase images of the chitin nanocrystal coating on the CA fibre at (c) 5 × 5 μm (d) 1.5 × 1. 5 μm.

3.2. Mechanical and thermal properties

The stress–strain curves and the tensile data of the electrospun membranes with and without chitin nanocrystal coating are given in Fig. 4 and Table 1. The results show that the impregnation of electrospun cellulose acetate with ChNC has positively influence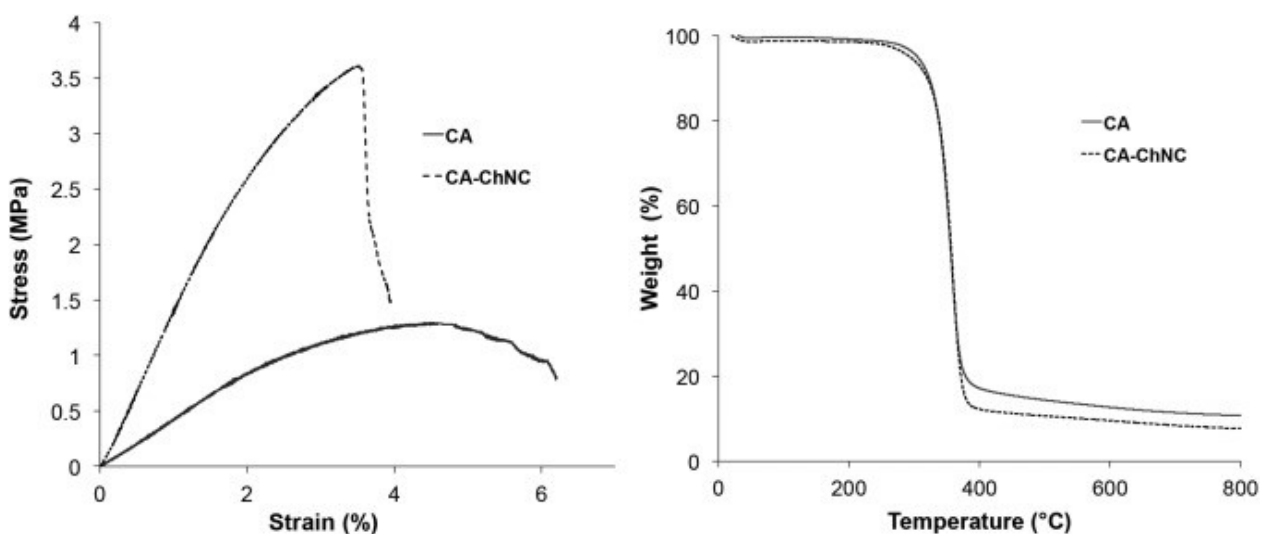d the tensile strength and E-modulus of the mats whereas the strain has decreased (Table 1). The tensile strength increased by 131 %, from 1.43 MPa to 3.31 MPa, while the E-modulus by 340 %, from 0.34 GPa to 1.16 GPa, with the infusion of 5% of ChNCs. The stress-stain behaviour also changed significantly after impregnation with a low amount of ChNCs.

This remarkable shift in mechanical performance can be attributed to the stiffening effect of the ChNCs coated on individual electrospun fibers as well as the mats in general (as evidenced by previous SEM images in Fig. 2, Fig. 3). The web formation at the fibre junctions 'ties' the electrospun fibers together, positively impacting the mechanical stability of the network. The strain at break however decreased as expected, which is attributable to the restricted slippage of the electrospun fibers past each other due to the 'tied' junction points. This so called "welding" or "soldering" of electrospun fibers, which enhance the bonding at junction points have been reported by some researchers [38-40]. To achieve this fusion of fibers, approaches such as the heating of the electrospun mats above the glass transition temperature but below the melting temperature of the polymer fibers [39-40] or solvent treatment of the electrospun mats are reported [38]. Huang et al. increased the TS of electrospun mats of polyacrylonitrile (PAN) by 500% (5–25 MPa) and polysulphone (PSu) 400-fold (0.8–3.2 MPa) via solvent treatment [38]. In this work, the chitin nanocrystals dried on the electrospun mats result in a similar 'welding' of the electrospun fibers with a relatively lower increase in mechanical TS (130%).

The thermal degradation behaviour showed a slight decrease in onset of thermal degradation temperature with the addition of the chitin nanocrystals from 304 °C to 293 °C (Fig. 4). This is attributable to the lower thermal stability of ChNCs compared to CA but will not compromise the use of the membranes in water purification [35].

Figure 4. The effect of ChNC coating on the mechanical properties and the thermal stability of CA electrospun fibers (a) stress–strain curves and (b) TGA curves are shown.

Table 1. Effect of chitin nanocrystals on the mechanical properties, thermal stability, and water flux of membranes.

	Tensile strength, MPa (±SD)	Strain, % (±SD)	Young's modulus, GPa (±SD)	T_{onset} °C	Flux, l m−2 h−1 (±SD)	Permeability
CA	1.43 (0.21)	6.23 (1.21)	0.34 (0.02)	304	13400 (700)	13300
CA-ChNC	3.31 (0.45)	3.42 (0.49)	1.16 (0.05)	293	14000 (300)	14100

3.3. Water flux and permeability

The water flux measurements (Table 1) show that the water flux at 0.5 bar and the permeability was not changed by the addition of the chitin nanocrystals. This high flux post-impregnation could be attributed to the hydrophilic nature of the CA-ChNC membrane while the surface coating of the cellulose acetate fibers where the chitin nanocrystals align along the cellulose acetate fibers first and then form webs between the fibers can influence flux and permeability. The high flux for the CA and CA-ChNC membranes is one of the attributes of these membranes that show promise in microfiltration applications, such as ready-to-eat vegetable process water. In comparison, Ma et al. have reported a flux of 5900 L m^{-2} h^{-1} bar^{-1} for PAN nanofiber mats impregnated with cellulose nanocrystals with a support layer [37] while our CA-ChNC membranes have a flux of 27 900 L m^{-2} h^{-1} bar^{-1}. This could be a result of our membranes having larger pore sizes, not requiring a support layer and the hydrophilicity of the cellulose acetate membrane in comparison to the PAN nanofibres.

3.4. Fouling behaviour

The flux variations of the membranes were evaluated to confirm the anti-fouling potential of the CA-ChNC membranes and to determine what effect the chitin nanocrystals would have on the abiotic fouling of the membranes. The change in flux was determined over 60 min of dead-end cell filtration. As can be seen in Fig. 5, the flux of the CA membranes steadily decreased over time as either 2 g/L bovine serum albumin or 0.5 g/L humic acid solutions were continually passed over the membrane. In comparison, the flux of the CA-ChNC membranes remained constant over the 60 min test period. While both membranes showed a decrease from the pure water flux upon initial contact with the membranes, after that initial contact the flux remained high and steady for the chitin nanocrystals coated membranes. These results indicate a promising potential for this type of membrane for future applications and further evaluation.

As biofouling is always a consideration in membrane applications, the use of chitin nanocrystals as inhibitors of such biofouling on the surface structure of these cellulose acetate fibre mats was considered. Biofilm formation was utilized to evaluate biofouling on chitin nanocrystals impregnated electrospun cellulose acetate. Fig. 6, Fig. 7 shows, respectively, SEM micrographs and Ruby FilmTracer confocal images of mats kept in contact for 18 and 24 h with cultures of *E. coli* CECT 516. In all cases the cellulose acetate membrane infused with chitin nanocrystals demonstrated significant resistance to be colonized by E. coli (Figs. 6b and 7b and f) in comparison to the electrospun cellulose acetate membranes (Figs. 6a, 7a and e), with a 48 % decrease in biofilm formation after 18 h and with a 87.7 % decrease after 24 h of incubation, according to the results obtained with FDA (Table 2)
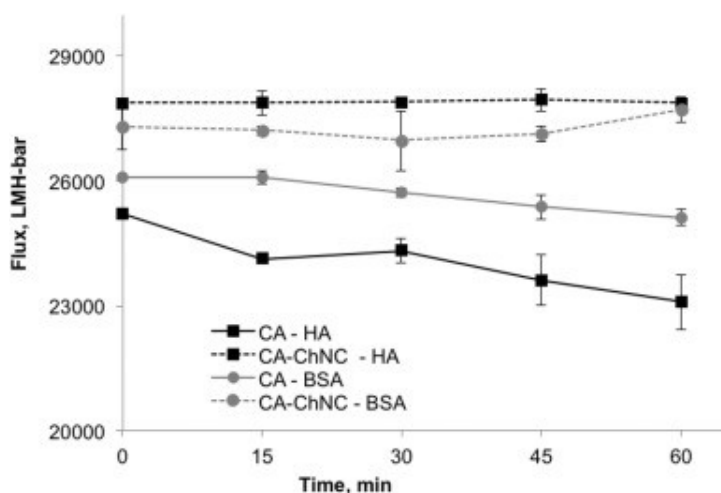

Figure 5. Flux variation as a function of time using crossflow filtration through CA and CA-ChNC membranes using water contaminated with humic acid and bovine serum albumin.
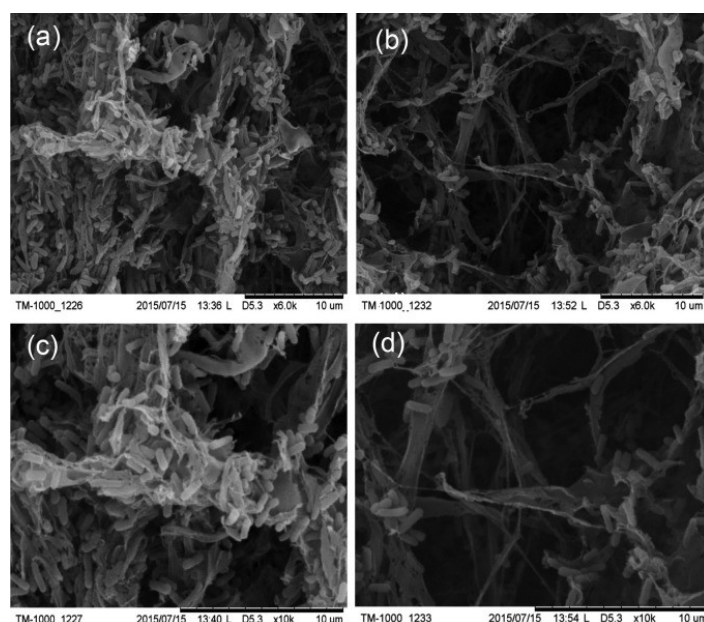

Figure 6. SEM micrographs of electrospun mats of CA (a and c) and CA- ChNC (b and d) in contact (18 h) with cultures of *E. coli* CECT 516.
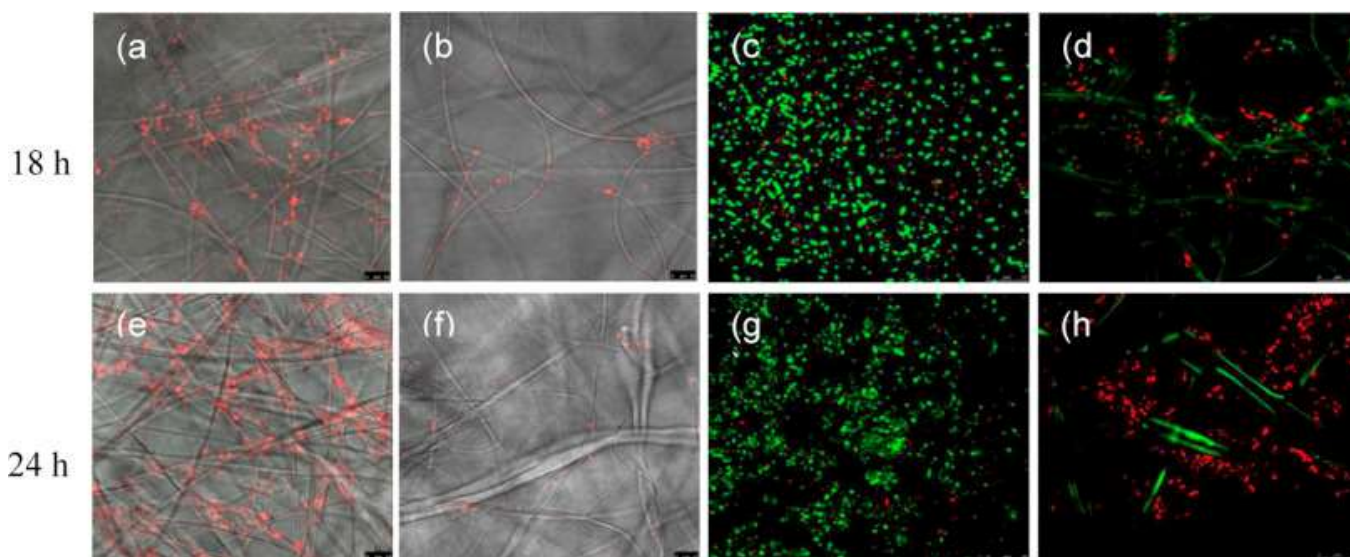
Figure 7. FilmTracer SYPRO Ruby biofilm matrix staining (a, b, e and f) and Live/Dead double staining (c, d, g and h) of *E. coli* CECT 516 on mats of CA (a, c, e and g) and CA-ChNC (b, d, f and h) after 18 h (a–d) and 24 h (e–h) of biofilm incubation.

Table 2. The effect of chitin nanocrystals on the ζ-potential, biofilm formation and contact angle of the electrospun membranes.

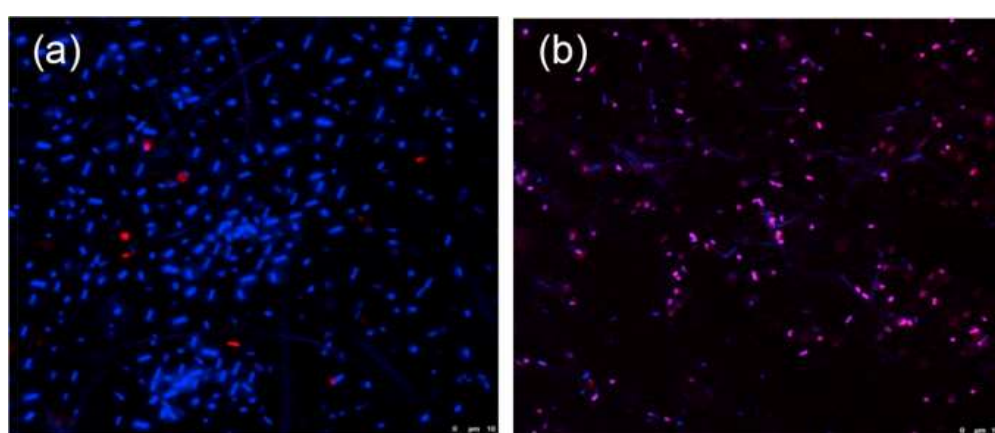|	ζ-potential (pH 7.5, mV) ($\pm$ SD)	FDA relative biofilm formation (18 h) ($\pm$ SD)	FDA relative biofilm Formation (24 h) ($\pm$ SD)	Contact angle, deg ($\pm$ SD)	
CA	−30.2 (1.8)	1 (0.04)	1.38 (0.07)	136.8 (3.6)	
CA-ChNC	−4.7 (2.5)	0.52 (0.03)	0.17 (0.09)	0.0 (0.0)	

Figure 8. DAPI/PI double staining of Escherichia coli CECT 516 on mats of CA (a) and CA-ChNC (b) after 18 h of cultures in contact with mats. Bacterial nuclei were visualized in blue by DAPI. Dead cells were stained in red by PI.

The results of FDA staining showed a much higher enzymatic activity of *E. coli* on raw CA membranes than on ChNC specimens. The higher number of PI-marked, non-viable cells on ChNC membranes is also apparent when comparing Fig. 7c–h. After 24 in contact with membranes, the viability of bacterial cell became notably reduced with most cells damaged. The differential staining with Ruby FilmTracer revealed the protein network of extracellular substances providing the mechanical stability of biofilms. Furthermore, with increasing incubation time, we observed an increase of extracellular matrix formation which would indicate a

8

biofilm proliferation on CA membranes, while on CA-ChNC this formation was considerably lower, revealing a reduced biofouling (Fig. 7). The results of DAPI/PI double staining is shown in Fig. 8. In this system, all cells exhibit blue (DAPI) fluorescence due to nucleus staining, whereas nonviable bacterial cells display red fluorescence (Propidium iodide, PI) with dye uptake depending on cell membrane integrity and physiological state of the bacterial cells. Again, the antibacterial activity of CA-ChNC is apparent in comparison with non-coated CA.

A possible explanation of this behaviour is the antimicrobial activity of chitin. Chitin and derivatives as chitosan have been investigated as an antimicrobial material against a wide range of target organisms like algae, bacteria, yeasts and fungi. Several models have been proposed, the most acceptable being the interaction between positively charged chitin/chitosan molecules and negatively charged microbial cell membranes. In this model the interaction was mediated by the electrostatic forces between protonated $-NH_3^+$ groups and the negative residues, presumably by competing with Ca^{2+} for electronegative sites on the membrane surface. This electrostatic interaction results in twofold interference: i) by promoting changes in the properties of membrane wall permeability, inducing internal osmotic imbalances and the inhibition of microbial growth and ii) by the hydrolysis of the peptidoglycans in the microorganism wall, leading to the leakage of intracellular electrolytes such as potassium ions and other low molecular weight proteinaceous constituents [41].

The formation of a biofilm includes several steps, but a prerequisite is the adhesion of microbial cells to a solid surface. Studies of bacterial adhesive properties have indicated that several cell surface physico-chemical factors contribute to the process of adhesion. Such factors include cell surface hydrophobicity, the presence of extracellular polymers and cell surface charge. The latter determines the electrostatic interaction between the cell and the substratum [42].

The value of the contact angle gives the basic information on the hydrophobicity of surfaces. For CA and CA-ChNC membranes water contact angles are given in Table 2. The cellulose acetate membrane had a hydrophobic contact angle of 136.8° while the CA-ChNC membranes demonstrated extreme hydrophilicity with a measured contact angle of 0°, since all the water drop was absorbed by the membrane. The contact angles are dependent upon the chemical composition, porosity, and surface roughness and hydrophilicity increases with the presence of N, O, I, Cl, H, and F. The chemical structure of the chitin nanocrystals on the surface of cellulose acetate (Fig. 1) is contributing to the dramatic reduction in the contact angle [26], [34][26], [31]. Generally, hydrophobic bacteria adhere on hydrophobic surfaces, whereas hydrophilic microorganisms attach to hydrophilic surfaces. The

interaction between two hydrophobic entities (*E. coli* cells and CA membranes in our case) is favoured because they can get closer contact through the facilitated "squeezing of water" in between, but the bio-surface interactions are somewhat more complex due to cell appendages, such as pili and flagella that makes direct contact between surfaces quite difficult [43].

The ζ-potential of the membranes is shown in Table 2. All membranes were negatively charged. CA membranes reached a surface potential of -30.2 mV whereas the CA-ChNC membranes displayed a ζ-potential of -4.7 mV at pH 7.5. As with contact angle, the chemical structure of the chitin nanocrystals on the surface of cellulose acetate (Fig. 1) is changing the surface properties of the CA membrane, making it less negative. Electrostatic repulsion could be expected to play a role in bacterial adhesion, given the negative surface charge of bacterial outer membranes (the ζ-potential of *E. coli* is approx. -30 mV) [44]. The data show, however, that the more negatively charged surfaces were more prone to suffer bacterial colonization as revealed by FDA (Table 2), FilmTracer and Live/Dead (Fig. 6) staining and by SEM imaging (Fig. 5). It has also been shown that some bacteria could interact with negatively charged particles if they bind to cationic sites on the cell surface to form clusters favoured by the repulsive interactions with negatively charged domains [45], [46].

Summarizing, besides the antimicrobial activity of chitin, the hydrophilic CA-ChNC membranes were much more resistant to bacterial colonization than unmodified CA mats. The possibility to convert highly hydrophobic membrane surfaces into superhydrophilic surface via surface functionalization with ChNC is also expected to open new possibilities in membrane technology. The membrane selectivity/rejection based on size exclusion and/or adsorption is of relevance in this context and will be reported in detail in future.

4. Conclusions

Chitin nanocrystals were successfully infused on to the electrospun cellulose acetate fibre networks resulting in a novel and highly efficient surface treatment approach for low-fouling membrane processing. The hierarchical morphology is shown by the membranes where micron scaled electrospun fibre network is surface coated with ChNC networks in nanoscale with pore sizes in the range on 10 nm. The ChNC coating on individual CA fibers that are 'tied' together at junction points by chitin nanocrystals webs increased the mechanical strength and modulus of the membranes. Addition of the chitin nanocrystals on the CA membrane surfaces resulted in decreased biofilm formation and abiotic fouling tendency accompanied with a transition from highly hydrophobic to super-hydrophilic surfaces. This is attributable to surface chemistry chitin nanocrystals and surface interactions of cellulose acetate membrane and *E. coli* cells. Chitin nanocrystals on cellulose acetate mats thus resulted in high flux membranes which shows

potential in future water purification of process wash water from food industry containing biological and organic contaminants.

Acknowledgments

References

[1] J. Cooley, Apparatus for Electrically Dispersing Fluids, US Patent Specification, 692631, 1902.

[2] W.J. Morton, Method of Dispersing Fluids, 1902.

[3] F. Anton, Process and Apparatus for Preparing Artificial Threads, 1934.

[4] D. Li, Y. Xia, Electrospinning of nanofibers: reinventing the wheel? Adv. Mater., 16 (2004), p. 1151.

[5] W. Teo, S. Ramakrishna. A review on electrospinning design and nanofibre assemblies Nanotechnology, 17 (2006), p. R89

[6] Z. Huang, Y. Zhang, M. Kotaki, S. Ramakrishna, A review on polymer nanofibers by electrospinning and their applications in nanocomposites. Compos. Sci. Technol., 63 (2003), p. 2223.

[7] Z. Ma, M. Kotaki, S. Ramakrishna, Electrospun cellulose nanofiber as affinity membrane. J. Membr. Sci., 265 (2005), p. 115.

[8] H.Y. Chung, J.R. Hall, M.A. Gogins, D.G. Crofoot, T.M. Weik, Polymer, Polymer Microfiber, Polymer Nanofiber and Applications Including Filter Structures, 2004.

[9] H. Hou, J.J. Ge, J. Zeng, Q. Li, D.H. Reneker, A. Greiner, S.Z.D. Cheng. Electrospun polyacrylonitrile nanofibers containing a high concentration of well-aligned multiwall carbon nanotubes. Chem. Mater., 17 (2005), p. 967.

[10] X. Wang, K. Zhang, M. Zhu, B.S. Hsiao, B. Chu, Enhanced mechanical performance of self-bundled electrospun fiber yarns via post-treatments. Macromol. Rapid Commun., 29 (2008), p. 826.

[11] R. Sen, B. Zhao, D. Perea, M.E. Itkis, H. Hu, J. Love, E. Bekyarova, R.C. Haddon, Preparation of single-walled carbon nanotube reinforced polystyrene and polyurethane nanofibers and membranes by electrospinning. Nano Lett., 4 (2004), p. 459.

[12] W. Park, M. Kang, H. Kim, H. Jin, Electrospinning of poly (ethylene oxide) with bacterial cellulose whiskers. Macromol. Symp, 249 (2007), p. 289.

[13] O.J. Rojas, G.A. Montero, Y. Habibi, Electrospun nanocomposites from polystyrene loaded with cellulose nanowhiskers. J. Appl. Polym. Sci., 113 (2009), p. 927.

[14] C. Xiang, Y.L. Joo, M.W. Frey, Nanocomposite fibers electrospun from poly (lactic acid)/cellulose nanocrystals. J. Biobased Mater. Bioenergy, 3 (2009), p. 147.

[15] J. Baker, L. Dudley, Biofouling in membrane systems –A review. Desalination, 118 (1998), p. 81.

[16] H. Flemming, G. Schaule, T. Griebe, J. Schmitt, A. Tamachkiarowa, Biofouling – the Achilles heel of membrane processes. Desalination, 113 (1997), p. 215.

[17] K.J. Howe, M.M. Clark, Fouling of microfiltration and ultrafiltration membranes by natural waters. Environ. Sci. Technol., 36 (2002), p. 3571.

[18] D. Rana, T. Matsuura, Surface modifications for antifouling membranes. Chem. Rev., 110 (2010), p. 2448.

[19] D. Klemm, F. Kramer, S. Moritz, T. Lindström, M. Ankerfors, D. Gray, A. Dorris, Nanocelluloses: a new family of nature-based materials. Angew. Chem. Int. Ed., 50 (2011), p. 5438.

[20] R.J. Moon, A. Martini, J. Nairn, J. Simonsen, J. Youngblood, Cellulose nanomaterials review: structure, properties and nanocomposites. Chem. Soc. Rev., 40 (2011), p. 3941.

[21] S.J. Eichhorn, Cellulose nanowhiskers: promising materials for advanced applications. Soft Matter, 7 (2011), p. 303.

[22] N. Herrera, A.P. Mathew, L. Wang, K. Oksman, Randomly oriented and aligned cellulose fibres reinforced with cellulose nanowhiskers, prepared by electrospinning. Plast. Rubber Compos., 40 (2011), p. 57.

[23] Z. Karim, A.P. Mathew, M. Grahn, J. Mouzon, K. Oksman, Nanoporous membranes with cellulose nanocrystals as functional entity in chitosan: removal of dyes from water. Carbohydr. Polym., 112 (2014), p. 668.

[24] A. Dufresne, Polysaccharide nano crystal reinforced nanocomposites. Can. J. Chem., 86 (2008), p. 484.

[25] N. Naseri, C. Algan, V. Jacobs, M. John, K. Oksman, A.P. Mathew, Electrospun chitosan-based nanocomposite mats reinforced with chitin nanocrystals for wound dressing. Carbohydr. Polym., 109 (2014), p. 7.

[26] N. Naseri, A.P. Mathew, L. Girandon, M. Fröhlich, K. Oksman, Porous electrospun nanocomposite mats based on chitosan–cellulose nanocrystals for wound dressing: effect of surface characteristics of nanocrystals. Cellulose, 22 (2015), p. 521.

[27] A.P. Mathew, M.G. Laborie, K. Oksman, Cross-linked chitosan/chitin crystal nanocomposites with improved permeation selectivity and pH stability. Biomacromolecules, 10 (2009), p. 1627.

[28] H-C. Flemming, Microbial Biofouling: Unsolved problems, insufficient approaches and possible solutions, in H-C. Flemming et al. (eds.), Biofilm Highlights, Springer Series on Biofilms 5, 81, Springer-Verlag, 2011, pp. 81–109.

[29] T.R. Garrett, M. Bhakoo, Z. Zhang, Bacterial adhesion and biofilms on surfaces. Prog. Nat. Sci., 18 (2008), p. 1049.

[30] M.E. Davey, G.A. O'Toole, Microbial biofilms: from ecology to molecular genetics. Microbiol. Mol. Biol. Rev., 64 (2000), p. 847.

[31] M. Rinaudo, Chitin and chitosan: properties and applications. Prog. Polym. Sci., 31 (2006), p. 603.

[32] K. Gopalan Nair, A. Dufresne, Crab shell chitin whisker reinforced natural rubber nanocomposites. 1. Processing and swelling behavior. Biomacromolecules, 4 (2003), p. 657.

[33] R. Marchessault, F. Morehead, N. Walter, Liquid Crystal Systems From Fibrillar Polysaccharides, 1959.

[34] A. Qin, X. Li, X. Zhao, D. Liu, C. He, Preparation and characterization of nano-chitin whisker reinforced PVDF membrane with excellent antifouling property. J. Membr. Sci., 480 (2015), p. 1.

[35] P. Liu, H. Sehaqui, P. Tingaut, A. Wichser, K. Oksman, A.P. Mathew, Cellulose and chitin nanomaterials for capturing silver ions (Ag) from water via surface adsorption. Cellulose, 21 (2014), p. 449.

[36] H. Ma, B.S. Hsiao, B. Chu, Ultrafine cellulose nanofibers as efficient adsorbents for removal of UO22 in water. ACS Macro Lett., 1 (2011), p. 213.

[37] H. Ma, C. Burger, B.S. Hsiao, B. Chu, Nanofibrous microfiltration membrane based on cellulose nanowhiskers. Biomacromolecules, 13 (2011), p. 180.

[38] L. Huang, S.S. Manickam, J.R. McCutcheon, Increasing strength of electrospun nanofiber membranes for water filtration using solvent vapor, J. Membr. Sci., 436 (2013), p. 213.

[39] S. Kaur, Z. Ma, R. Gopal, G. Singh, S. Ramakrishna, T. Matsuura, Plasma-induced graft copolymerization of poly (methacrylic acid) on electrospun poly (vinylidene fluoride) nanofiber membrane. Langmuir, 23 (2007), p. 13085.

[40] R. Gopal, S. Kaur, Z. Ma, C. Chan, S. Ramakrishna, T. Matsuura, Electrospun nanofibrous filtration membrane. J. Membr. Sci., 281 (2006), p. 581.

.

[41] R.C. Goy, Dd Britto, O.B. Assis, A review of the antimicrobial activity of chitosan. Polímeros, 19 (2009), p. 241.

[42] J. Azeredo, R. Oliveira, The role of hydrophobicity and exopolymers in initial adhesion and biofilm formation. Piet Lens, Anthony P. Moran, Therese Mahony, Paul Stoodley, Vincent O'Flaherty (Eds.), Biofilms Biofilms in Medicine, Industry and Environmental Biotechnology, IWA Publishing, London (2003), pp. 16-31.

[43] K. Hori, S. Matsumoto, Bacterial adhesion: from mechanism to control. Biochem. Eng. J., 48 (2010), pp. 424-434.

[44] Y.L. Ong, A. Razatos, G. Georgiou, M.M. Sharma, Adhesion forces between *E. coli* bacteria and biomaterial surfaces. Langmuir, 15 (1999), pp. 2719-2725.

[45] A. Dasari, J. Quirós, B. Herrero, K. Boltes, E. García-Calvo, R. Rosal, Antifouling membranes prepared by electrospinning polylactic acid containing biocidal nanoparticles. J. Membr. Sci., 405–406 (2012), pp. 134-140.

[46] C. Wilhelm, C. Billotey, J. Roger, J.N. Pons, J.C. Bacri, F. Gazeau, Intracellular uptake of anionic superparamagnetic nanoparticles as a function of their surface coating. Biomaterials, 24 (2003), pp. 1001-1011